Journal of Cleaner Production 423 (2023) 138742

Contents lists available at ScienceDirect

Journal of Cleaner Production

journal homepage: www.elsevier.com/locate/jclepro

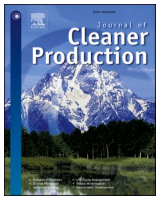

Towards a low-carbon future for offshore oil and gas industry: A smart integrated energy management system with floating wind turbines and gas turbines

Reyhaneh Banihabib *, Mohsen Assadi

University of Stavanger, Stavanger, Norway

ARTICLE INFO

Handling Editor: Panos Seferlis

Keywords:
Decarbonization
Offshore microgrid
Floating wind turbines
Hydrogen-compatible gas turbines
Hybrid optimization
Online optimization
AI algorithms
Operational efficiency
Sustainable energy future
Carbon-based emissions

ABSTRACT

Decarbonizing offshore oil and gas fields is crucial in the global fight against climate change. To achieve this objective, the offshore oil and gas industry has embraced innovative energy systems, including microgrids that seamlessly integrate renewable energy sources like floating wind turbines. This study presents a comprehensive investigation into an integrated energy management system for an offshore microgrid, encompassing three platforms and a floating wind farm, along with green hydrogen production and storage facilities.

The operational decision-making process for such a complex microgrid, involving numerous assets, presents notable challenges. To address this, a sophisticated smart management system is employed, enabling efficient optimization with advanced forecasting capabilities to identify the most cost-effective and environmentally friendly version of the microgrid's operation. To overcome the intricacies of optimization and computational constraints, a novel hybrid optimization approach, with a platform-centric strategy, is utilized. Leveraging real-world operational data, the study harnesses an innovative online optimization method fortified with state-of-the-art AI algorithms.

The results of the optimization are benchmarked against a rule-based operation, wherein no formal optimization occurs, but the most economically viable decisions are made. The findings underscore the effectiveness of the developed optimization method, leading to a significant 16% reduction in operational costs and carbon-based emissions compared to the rule-based approach.

This study effectively demonstrates the real-world applicability of the developed method by applying and testing the smart management system on an actual offshore platform with minimal simplifications. The investigation provides valuable evidence of the method's adaptability to complex operational scenarios, highlighting its potential for practical implementation in the offshore oil and gas industry.

1. Introduction

The extraction and processing of fossil fuels significantly impact the release of greenhouse gases (GHGs), highlighting the urgency to find effective strategies for minimizing these emissions and achieving a carbon-neutral society. Offshore facilities rely heavily on gas turbines (GTs) for power generation, using natural gas or diesel oil as fuels, thereby being the primary sources of CO_2 and NOx emissions. According to a report, in 2022, GTs accounted for 81% of CO_2 emissions generated by petroleum activities in the Norwegian Continental Shelf (NCS) (Norwegian Petroleum Directorate, 2023). The power required on oil and gas (O&G) platforms ranges from 10 MW to several hundreds of MW, depending on factors like temperature, pressure, and field properties (Polleux et al., 2022). To meet this demand GTs coupled with electric generators operate by burning natural gas or diesel oil (Zhang et al., 2018).

Dependence on GTs for power generation in offshore O&G facilities significantly amplifies environmental consequences. The continuous release of CO_2 intensifies the global issue of climate change (Hachem et al., 2022), setting off a series of effects. These include the gradual increase in global temperatures, rising sea levels, and disruptions to ecosystems. The long-term consequences of GHG emissions not only affect the local marine environments around offshore installations but also contribute to broader climate shifts (Grasso, 2019), underscoring

* Corresponding author.
E-mail addresses: Reyhaneh.Banihabib@uis.no (R. Banihabib), Mohsen.Assadi@uis.no (M. Assadi).

https://doi.org/10.1016/j.jclepro.2023.138742
Received 16 June 2023; Received in revised form 27 August 2023; Accepted 7 September 2023
Available online 12 September 2023

the need for a comprehensive and globally oriented response (International Energy Agency, 2020). In response to environmental concerns, the offshore O&G industry is experiencing a transformative shift driven by evolving regulations, societal pressures, and a growing recognition of its environmental footprint. International efforts like the Paris Agreement illustrate the joint commitment to reducing emissions and controlling global warming (Haszeldine et al., 2018). The International Maritime Organization and its Energy Efficiency Existing Ship Index regulations demonstrate global initiatives to limit emissions in the maritime sector, which also influence offshore operations (Watson, 2020).

Norway has been a pioneer in promoting environmental awareness and reducing GHG from the O&G sector. In 1991, Norway introduced a CO_2 tax of approximately 40 €/ton. Over time, the implementation of this policy has resulted in operators on the NCS now facing a combined CO_2 tax of 52 €/ton, which is expected to increase to more than 70 €/ton by 2040 due to the tightening of regulatory frameworks in Europe (Oliveira-Pinto et al., 2019). The European Union Trading System (ETS), created in 2005, has also significantly promoted environmental awareness, with current ETS prices around 5 €/ton of CO_2 (Oliveira-Pinto et al., 2019). As a result, the increasing emissions of GHGs not only pose environmental concerns but also result in significant financial penalties. Therefore, improving the energy management of offshore facilities is becoming an economic driver for the industry (Oliveira-Pinto et al., 2019). Particularly in Norway, where the cost of CO_2 emissions stemming from natural gas utilization in petroleum fields is notably high at approximately 2400 NOK/ton of natural gas (equivalent to about 214 €/ton) under the 2023 regulatory framework ("Tax rates in Norway), field operators have shown keen interest in exploring solutions to reduce O&G platform emissions.

One of the strategies embraced by O&G facilities in Norway to attain sustainability and decrease emissions is adopting onshore power sources. Given that a substantial portion of onshore power in Norway is derived from renewable sources (International Energy Agency, 2022), this approach is gaining momentum. Currently, 16 fields have either already implemented or are planning to use this technology (Norwegian Petroleum Directorate Professor Olav Hanssens and vei, 2020), which is projected to account for around 45% of total O&G production on the continental shelf (Norwegian Petroleum Directorate Professor Olav Hanssens and vei, 2020). This shift towards power from land solutions is expected to significantly reduce petroleum-related emissions in Norway, avoiding approximately 3.2 million tons of CO_2 emissions annually-equivalent to a quarter of the total emissions from the petroleum sector in 2019 (Norwegian Petroleum Directorate Professor Olav Hanssens and vei, 2020).

Another avenue showing promise in mitigating emissions within the offshore sector is CO_2 capture and storage (CCS) from turbine exhaust. Despite its potential, the practical implementation of this method on platforms presents intricate logistical challenges that necessitate careful consideration. The need for substantial infrastructure in proximity to the gas turbine, combined with spatial constraints on these platforms, complicates the approach (Roussanaly et al., 2019). Consequently, exploring innovative solutions characterized by compactness and reduced weight becomes essential, bypassing the hurdles posed by spatial limitations and heavy equipment installation (Anekwe et al., 2023). Despite the challenges, significant progress has been achieved in implementing CO_2 capture from turbine exhaust on offshore platforms, exemplified by the United Kingdom and Norway ("Carbon capture and storage, 2023). This uptake validates the technology's feasibility in the offshore environment. Other than Europe, the initiatives in offshore carbon dioxide storage in regions such as the United States, Japan, and Australia, underscore a commitment to safe and environmentally responsible storage, complemented by their respective regulations and policies (Luo et al., 2023).

The integration of renewable energy sources and alternative power supply methods is another avenue to address the challenges of sustainable offshore operations. This approach offers a multifaceted solution to the challenges of sustainable offshore operations. Renewable energy sources, including wind, solar, and wave energy, have gained traction as effective tools to reduce the carbon footprint of offshore O&G platforms (de Souza et al., 2022). Wind turbines, in particular, stand out due to their suitability for offshore high wind speeds. Developing hybrid energy systems that combine renewable sources with conventional gas turbines aims to enhance offshore platform efficiency and sustainability, ensuring a consistent power supply to meet operational demands. This integration leads to substantial contributions to energy demand through renewables, resulting in emissions reduction and notable cost savings (Watson, 2020). While the shift to renewable energy sources may entail upfront expenses, the reduction in operational costs and avoidance of emissions-related taxes can lead to significant economic benefits (International Renewable Energy Agency (IRENA), 2019). Government incentives and regulatory support play a pivotal role in shaping the economic landscape of this transition (International Renewable Energy Agency (IRENA), 2019).

Insights into the growth of offshore wind in the Asia Pacific region and the policies implemented by various governments to promote this sector are provided in (Cheng and Hughes, 2023). The operation of a 4 $\times$ 5 MW offshore wind farm operating in parallel with GTs was studied by Korpås et al. (2012). The findings highlight the potential for significant cost savings and emissions reductions, validating the viability of offshore wind integration for sustainable and efficient power supply to O&G field centers. Zhang et al. (2021) explored the integration of wind power into offshore O&G field energy systems, assessing its economic and environmental performance. According to the authors (Zhang et al., 2021), introducing wind energy reduced carbon emissions by approximately 39.91% and lowered the total annual cost by about 2.57% (Zhang et al., 2021).Additionally, Panda et al. investigated an XAI-driven net-zero carbon roadmap for the petrochemical industry, considering stochastic scenarios of offshore wind energy, which demonstrated the potential for further advancements in cost reductions and emissions mitigation through the integration of renewable energy sources (Panda and Das, 2021).

Although the benefits of integrating renewable energy sources, particularly wind power, are evident, its intermittent nature introduces technical challenges causing system instability, potentially requiring a reliable backup power source (Al-Shetwi, 2022). To that end, the incorporation of energy storage and energy management systems becomes imperative in the integrated system. Notably, the offshore wind sector is undergoing rapid global expansion since it holds the dual promise of decarbonizing electricity and serving as a platform for hydrogen production, thus addressing energy storage needs (Durakovic et al., 2023). This concept involves generating green hydrogen through electrolysis technology by converting water into hydrogen using surplus renewable energy. The stored hydrogen can then serve as carbon-free fuel for gas turbine units. The utilization of hydrogen and hydrogen-based fuels has gained attention for gas turbines in recent decades and many original equipment manufacturers have shared information regarding the hydrogen compatibility of their engines (Amin and Fors, 2020), (Goldmeer, 2019).

Researchers have investigated the feasibility of producing and utilizing green hydrogen on offshore platforms by harnessing available wind power to run an electrolyzer, converting water, readily abundant in offshore fields, into hydrogen (Dokhani et al., 2023), (Riboldi et al., 2020). In (Kumar et al., 2023), the authors offered valuable insights into the symbiotic relationship between the green hydrogen sector and offshore industries. Their analysis of integrating offshore renewable energy systems with O&G sectors revealed the advantages, contributions, and safety considerations of green hydrogen in decarbonizing offshore industries (Kumar et al., 2023). Giampieri et al. (Giampieri et al., 2023) show that producing green hydrogen from offshore wind could achieve significant cost reduction by 2030 and 2050, making it competitive against grey and blue hydrogen. According to their study,

compressed hydrogen production offshore is the most cost-effective scenario for projects starting in 2025, while alternative strategies like liquefied hydrogen or methylcyclohexane may become more cost-effective for projects beginning in 2050 (Giampieri et al., 2023). Riboldi et al. compared three offshore energy supply models: standard gas turbines, a hybrid GT-wind turbine setup, and a hybrid energy system for offshore integrating GTs, WTs, and hydrogen storage (Riboldi et al., 2020). Results reveal the third approach's potential to notably cut CO_2 emissions (up to 40%) compared to conventional setups, supported by an optimization framework for sustainable offshore energy solutions (Riboldi et al., 2020).

To power offshore rigs sustainably, a hybrid energy system that combines offshore wind power, on-site gas turbines, and power-to-gas storing electrolyzers becomes a necessary solution. Integrating these diverse energy sources and technologies is imperative to transform various offshore drilling and production platforms into integrated energy microgrids (IEMs) that can interact effectively with offshore power plants (Li et al., 2022). The criteria for a microgrid include having a well-defined electrical boundary, a control system for resource management, and a generation capacity exceeding critical load to allow the microgrid to operate independently from the main grid (Li et al., 2020). Implementing smart IME can optimize the use of diverse energy sources, minimize waste, and improve system reliability for the sustainable development of offshore O&G platforms. These advanced energy management systems facilitate decarbonization efforts, enable remote monitoring, reduce human intervention, and enhance overall safety.

The offshore microgrid concept has been extensively studied (Grainger et al., 2021; Adrian, 2022; Peters et al., 2020; Ventrelli, 2022), with most research concentrating on evaluating the feasibility and analyzing renewable integration in O&G fields. Some studies targeted power balancing for IEM systems and addressed the challenges of assuring power demand satisfaction (Anglani et al., 2020; Yu et al., 2020; Zare et al., 2023; Jing et al., 2022). The literature also addresses the significance of operational strategies and system integration involving offshore wind farms and gas turbines on platforms for achieving emission reductions (Svendsen et al., 2022).

This study goes beyond ensuring power demand and production balance, by introducing a smart energy management system that optimizes asset operation in the microgrid to reduce costs and emissions. Furthermore, the development of an online platform with highly accurate models for optimizing offshore microgrid operation is a novel practice, yet to be conducted as per the authors' knowledge. Additionally, while the concept of offshore microgrids in a theoretical context has been covered in the literature (Panda and Das, 2021), (Zare et al., 2023), (Li et al., 2023) this study delves into a real-world scenario, analyzing an actual case with verifiable data. In line with the challenges posed by hybrid integrated energy systems, the incorporation of advanced optimization techniques and control strategies, as highlighted in (Shezan et al., 2023), could potentially enhance the effectiveness of the proposed smart energy management system.

The paper is organized as follows: first, a description of the offshore platform under study is presented, followed by the methodology for operating the platform conventionally versus using smart management tools. Lastly, the results of the operation in both scenarios are presented for a week of operation, demonstrating the value of using smart management systems for offshore IEMs.

2. Case study description

2.1. Gullfaks platforms and Hywind Tampen

The Gullfaks O&G field is situated in the Norwegian sector of the North Sea, at a latitude of 61.21 and a longitude of 2.27. The field comprises three platforms - Gullfaks A (GFA), Gullfaks B (GFB), and Gullfaks C (GFC) - all of which were constructed in the 1980s. These platforms serve the dual purpose of drilling and production, as well as accommodating personnel. Originally, these platforms were designed to operate using gas turbines; however, in line with the goal of reducing carbon emissions, Equinor, the field operator, has initiated a project to source a portion of the power needed for the platforms from a floating wind farm. Hywind Tampen is the first offshore wind farm that provides renewable energy to the offshore O&G field (Tampen - Equinor). The farm is designed to operate at a 125 km distance from the shore.

The floating wind farm consists of a total of 11 wind turbines, each of 8 MW capacity. Out of these 11 turbines, five are specifically allocated to generate power for the Gullfaks field, while the rest are intended to serve the Snorre field, another O&G field in the Norwegian sector of the North Sea (Norwegian Petroleum Directorate Professor Olav Hanssens and vei, 2020). The field operator has provided a visual representation, depicted in Fig. 1, to illustrate the positioning of the Hywind Tampen, Gullfaks, and Snorre fields. The field operator is currently exploring the feasibility of expanding the farm's capacity to 94.6 MW by upgrading the wind turbines.

Through the utilization of this floating wind farm to supply power to the Gullfaks and Snorre fields, it is projected that around 200,000 tons of CO_2 emissions and 1000 tons of NOx emissions can be omitted (Tampen - Equinor). Notably, the wind turbines will directly deliver electricity to the offshore oil platforms, without relying on any connections to the land. It is expected that these turbines will meet approximately 30–35% of the total energy demand across the five platforms (Adrian, 2022).

Hywind's design is based on a spar buoy, with a heavy sub-structure and a lighter upper structure to maintain stability. The Siemens SQT 8.0–154 turbine model has been chosen for the farm, featuring a hub height of 95 m, 3 blades with a diameter of 154 m, a nacelle weight of 480 tons, and a floater weight of 10,000 tons. Since Siemens has not disclosed the power curve for this specific model, the power curve for Vestas' V164–8.0 MW turbine was utilized. The relevant data for both Siemens and Vestas turbines are presented in Table 1 below. The similarity between the configuration and the operational parameters of these two models enables the use of operational data of V165–8.0 (available in (Desmond et al., 2016)) as a close estimation of SWT 8.0–154.

All the platforms are equipped with General Electric's LM2500 engines, which is an aero-derivative gas turbine with a power capacity of 22 MW. The GFA platform has four of these gas turbines installed, while the GFC platform has three. Each turbine, except one, on both platforms is equipped with a waste heat recovery unit (WHRU). GFB platform doesn't house any gas turbines and instead receives its required power from GFA through two sea cables, capable of transferring a maximum of 20 MW of power. GFA and GFC are also connected via a cable with the same power transmission limit. To supply power to the Gullfaks field using wind energy, there is a cable that connects the Hywind facility to GFA. Fig. 2 provides a visual representation of the fields and their interconnections.

The energy demand on the platforms encompasses essential needs such as lighting, heating for the accommodation spaces, accommodating 2–300 personnel, as well as computer and control systems responsible for platform management and communication. However, the primary power consumer is the O&G production process itself. Around 70% of the total onboard electrical power is dedicated to fulfilling the energy requirements of the production process consumers (Tangerås and Tveiten, 2018).

2.2. Adding storage system

Assuming the installed wind turbines cover 35% of the total demands on the platform, it is expected to reduce the emissions more with further installation of the wind turbines. However, a platform that could solely operate on wind farms is not feasible due to the intermittency of power generation from the wind. Adding a storage system, suitable to the condition and the environment, could mitigate problem. A microgrid serving as an integration of wind turbines, storage systems, and gas turbines could manage the demands of the field with the minimum

Fig. 1. The Hywind Tampen project and its connection to Gullfaks and Snorre fields ("Hywind Tampen approved by Norwegian), ("Views from the industry).

Table 1
Comparison of wind turbine models (Tangerås and Tveiten, 2018).

Parameter	Siemens SWT 8.0–154	Vestas V164–8.0
Diameter [m]	154	164
Area [m2]	18627	21124
No. of blades [-]	3	3
Cut-in wind speed [m/s]	3~5	4
Cut-out wind speed [m/s]	25	25
Nominal wind speed [m/s]	13~15	13
Nominal power [MW]	8	8

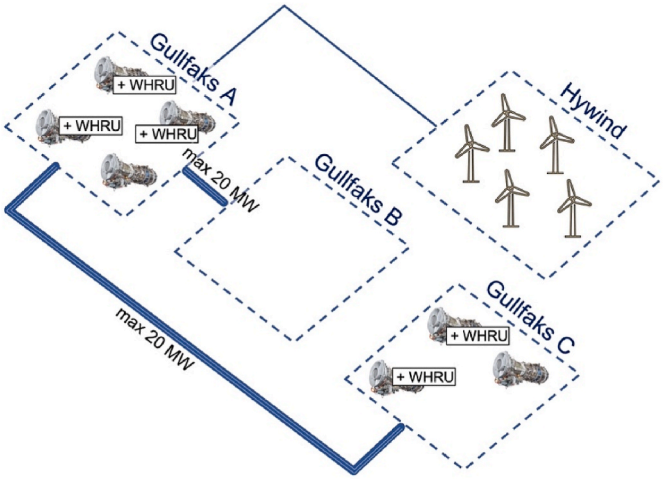

Fig. 2. Schematic view of Gullfaks platforms and Hywind wind farm with their connections.

emissions possible. The end goal is to reduce the operation of gas turbines with fossil fuel gas.

Various studies have extensively explored the feasibility and techno-economic aspects of green hydrogen production and local storage, specifically focusing on harnessing seawater and wind power (Dokhani et al., 2023), (Adrian, 2022). These investigations highlight the low cost associated with water desalination (Dokhani et al., 2023) and emphasized the economic viability of subsea storage of compressed hydrogen as a means to effectively store surplus wind power (Adrian, 2022).

To establish the necessary infrastructure for hydrogen production and storage, key components such as a saltwater desalination facility, feed water storage, electrolyzer, hydrogen compressor, hydrogen storage tanks, and the requisite transmission elements (including pipes and connections) between these components are essential (GREENSTAT). It is envisioned that a platform or floater will be required to accommodate the hydrogen production line, with the storage tanks positioned subsea. At present, the commercial availability of subsea hydrogen storage remains limited. However, ongoing initiatives led by Norwegian companies indicate promising developments in this field, with a focus on pressurized hydrogen tanks supported by a rigid structure capable of storing up to 12 tons of compressed hydrogen ("Hydrogen).

Given the existing connection of GFA with the wind turbines and the two other platforms (GFB and GFC), GFA serves as a pivotal junction in the microgrid setup. Consequently, it is proposed that the platform or floater be constructed in close proximity to GFA, housing the subsea hydrogen storage tanks. For the planned system, a stack comprising 15 proton exchange membrane electrolyzers, each boasting 6 MW capacity is considered. Relevant data relating to the electrolyzers can be found in (Kopp et al., 2017), while Fig. 3 provides the performance curve for each electrolyzer.

Regarding hydrogen storage, a capacity of 100 tons is deemed economically viable and reliable, as demonstrated by (Adrian, 2022). Occupying approximately 580 m^3 of space on the seabed, the pressurized hydrogen storage will be connected to GFA, facilitating an alternative fuel source for the gas turbines. While all the gas turbines on the platform are of the same model, this study assumes that only one of the turbines will be modified to operate on hydrogen-blended fuel, and the remaining turbines will continue to utilize natural gas as their conventional fuel source.

3. Microgrid operation management

For the operation of the Gullfaks field with power productions from Hywind farm, the seven gas turbines installed on GFA and GFC platforms and the electrolyzer and hydrogen storage are considered within a microgrid operation, running in island mode. The wind farm is assumed to increase its capacity to cover 100% of the field's operation and the storage system and gas turbines will help with mismatches of production and demand. Fig. 4 illustrates the Gullfaks microgrid's layout. A comprehensive control system oversees all microgrid components and manages their operation. The gas turbines' power output, the electrolyzer's power supply, and the hydrogen consumption are determined by the control system, with one of the gas turbines assumed to run with a hydrogen blend. The controller has to assure the balance of the demand and production (both power and heat) at each time step of the operation.

The management system ensures that the combined power output from the gas- and wind turbines adequately meets the power demand of

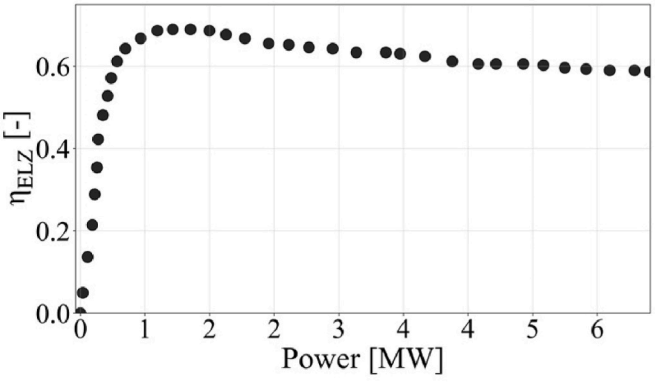

Fig. 3. The efficiency of hydrogen production as a function of the total power consumption of the electrolyzer (Kopp et al., 2017).

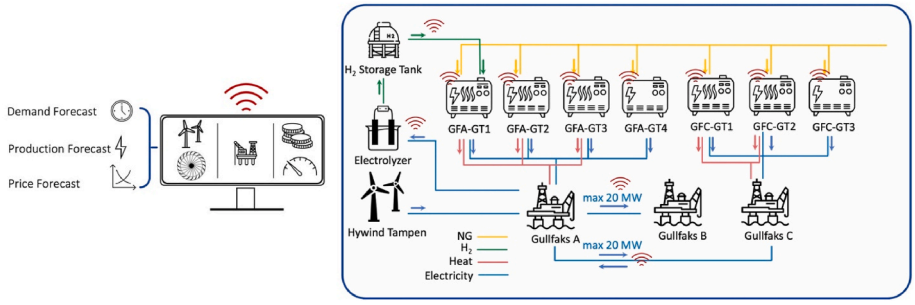

Fig. 4. Schematic diagram of the offshore microgrid and the smart management system.

each platform while also supplying power to the electrolyzer, in case of a surplus. The platforms require power and heat for essential operations and for running accommodations for personnel. The heating requirements of the facilities can be partially met by gas turbines equipped with WHRUs. Additionally, circulating water passes through an electrical heater to further warm it when the heating capacity of the gas turbines is insufficient or unavailable. For instance, on the GFB platform, which lacks a gas turbine, both the power and heat demands are fulfilled by GFA and transferred via a cable, since the heating demand on the GFB platform is addressed by an installed electrical heater.

At each time step, the operation decision made for the controllable units has to satisfy certain constraints regarding the conservation of power, heat, and hydrogen content. To write the energy balance for each platform, GFB could be conducted first as it has minimum connections to other platforms and has no energy production unit on it. The conservation of energy for platform GFB is shown in Eq. (1) to Eq. (3). All of the heat demand of GFB is provided by the electrical heater (Eq. (1)) and the power required to run it is calculated based on its efficiency (Eq. (2)), which is 85%. The power received from platform A should be equal to the demanded power and the power consumed by the electrical heater (Eq. (3)).

$$Q_{ELH\_GFB} - Q_{dem\_GFB} = 0 \tag{1}$$

$$P_{ELH\_GFB} = Q_{ELH\_GFB} / \eta_{ELH\_GFB} \tag{2}$$

$$P_{GFA\_GFB} - P_{dem\_GFB} - P_{ELH\_GFB} = 0 \tag{3}$$

The GFC platform also has a connection to GFA for which the power and heat conservation is written as below, in Eq. (4) to Eq. (6). The heat demands on GFC are met by the two gas turbines with WHRU, along with the utilization of an additional electrical heater on GFC (Eq. (4)). The electrical heater's power is calculated based on its efficiency (Eq. (5)). Finally the power balance of GFC is calculated, balancing the power generated by the gas turbines, the demanded power, the electrical heater's power, and the power transferred between GFA and GFC (Eq. (6)).

$$Q_{GFC\_GT1} + Q_{GFC\_GT2} + Q_{ELH\_GFC} - Q_{dem\_GFC} = 0 \tag{4}$$

$$P_{ELH\_GFC} = Q_{ELH\_GFC} / \eta_{ELH\_GFC} \tag{5}$$

$$P_{GFC\_GT1} + P_{GFC\_GT2} + P_{GFC\_GT3} + P_{GFA\_GFC} - P_{dem\_GFC} - P_{ELH\_GFC} = 0 \tag{6}$$

Lastly, the heat and power balance for GFA is analyzed by Eq. (7) to Eq. (9). The required heat demand is met by the implementation of three gas turbines equipped with WHRU, accompanied by an additional electric heater (Eq. (7)). The power consumption of the electrical heater is computed based on its efficiency (Eq. (8)), which is then integrated into the power balance equation (Eq. (9)). The power balance for GFA encompasses the generated power from the four gas turbines, the power supplied from the wind farm, and the consuming elements, including the electrolyzer's consumption, power transfers to GFB and GFC, as well as the power demand and electrical heater's consumption on the GFA platform (Eq. (9)).

$$Q_{GFA\_GT1} + Q_{GFA\_GT2} + Q_{GFA\_GT3} + Q_{ELH\_GFA} - Q_{dem\_GFA} = 0 \tag{7}$$

$$P_{ELH\_GFA} = Q_{ELH\_GFA} / \eta_{ELH\_GFA} \tag{8}$$

$$P_{GFA\_GT1} + P_{GFA\_GT2} + P_{GFA\_GT3} + P_{GFA\_GT4} + P_{WT} - P_{GFA\_ELZ} - P_{GFA\_GFB} - P_{GFA\_GFC} - P_{dem\_GFA} - P_{ELH\_GFA} = 0 \tag{9}$$

The power allocated to the electrolysis process (P_{GFA_ELZ}) serves multiple purposes, including water desalination, electrolysis operations, and pressurizing the stored hydrogen (Eq. (10)). To fulfill the desalination requirement of seawater, an energy input of 3.86 kJ per kilogram of seawater is considered (Lim et al., 2021). Additionally, with an adiabatic compression process and a compressor efficiency of 70%, the power consumed by the compressor amounts to 60 kJ per kilogram of hydrogen. Therefore, the complete process necessitates approximately 90 kJ of power for the production of 1 kg of hydrogen, which is obtained from 9 kg of seawater.

$$P_{GFA\_ELZ} = P_{ELZ} + P_{ds} + P_{comp} \tag{10}$$

An important aspect to consider is that the power transmission between GFA and GFC (P_{GFA_GFC}) is prone to power waste, due to the approximately 6 km distance between the platforms. While transmission in both directions is possible, around 0.11 MW are considered to be wasted for every megawatt of power leaving the platform. Therefore, when modeling and exploring different operation scenarios, special attention must be given to the direction of power transferred between GFA and GFC, as well as the value of the power term involved in the power balance of each platform. The power transferred from GFA to GFB (P_{GFA_GFB}), is also prone to 5.4% of waste due to the approximately 3 km distance between them. However, this power transfers in one direction, making it simpler to implement in the equations.

In addition to power and heat conservation, hydrogen conservation is also a critical consideration. Ensuring an adequate fuel supply for the gas turbines at the beginning of each time step is essential. Specifically, for GFA-GT1, the availability of hydrogen in the tank is crucial. Thus, the hydrogen required for consumption at each time step, denoted as t_i, must be less than the tank value accumulated from the initial condition to time step t_i. This constraint is represented by Eq. (11).

$$\left(m_{H_2,GFA-GT1}\right)_{t_i} < \left(M_{HyT}\right)_{t_0} + \sum_{t_o}^{t_i} M_{H_2,produced} - M_{H_2,consumed} \tag{11}$$

Ensuring heat and power conservation on each platform within the field is a constant requirement that must be met. However, variables such as the power output of gas turbines, the levels of hydrogen production and consumption, and the power transmission between platforms can fluctuate. These operational choices inherently lead to varying costs and emissions. There are two approaches to managing the operation:

- To follow certain rules which assure the balance of demand and production. This approach is called "condition-based". At each time step, the demands (power and heat on each of the three platforms) are declared and the wind power is determined. According to the condition, a decision is made to control the microgrid's operation.
- To predict the demands and renewable production ahead of time, and optimize the microgrid operation based on the forecasts. This approach is called "optimization", which searches for the best operational solution with minimum costs and emissions while assuring the demands are met.

In this study, both operation scenarios are thoroughly investigated and discussed. It is important to note that the condition-based operation does not involve optimization or forecasting tools; yet, decisions are based on a set of rules which aims to minimize costs as much as possible. This aspect is crucial to ensure a fair comparison with the optimizer's performance, as it would be unfair to compare it with an operator that does not make the best economical decision at each time step. The research demonstrates how the intelligent management system, i.e., the optimizer operation, can further enhance the overall operation compared to the already economical condition-based operation.

3.1. Scenario 1: condition-based operation

In this scenario, the Gullfaks microgrid follows a set of predefined rules to manage the assets. These rules provide immediate guidelines for operation based on real-time demand and the power generated by the wind turbine. The rules are designed with the following principles in mind:

- Platforms equipped with gas turbines (GFA and GFC) prioritize local power production over receiving power from connecting platforms. This approach minimizes unnecessary power transportation, which can lead to transmission losses.
- Each platform aims to minimize the number of gas turbines operating simultaneously. If the power demand of a platform can be met by two gas turbines instead of three, the two engines will operate at a higher load. This decision is driven by the fact that higher loads result in increased engine efficiency (Brenntrø, 2016).
- When multiple engines are required to meet the demand of a platform, the load is distributed equally among them to ensure balanced operation.
- The heat demand of the platforms is primarily fulfilled by the heat generated by the gas turbines. Utilizing the excess heat from gas turbines is more economical than using additional power for electrical heaters. In cases where the heating capacity is insufficient, an electrical heater is utilized to supplement the heat supply.
- The electrolyzer is only supplied with power if the power generated by the wind turbine exceeds the combined demand of platforms GFA and GFB. This ensures that excess renewable power is utilized for hydrogen production.
- If hydrogen is available, its consumption takes priority, limited to the availability of hydrogen reserves.

According to these principles, the condition-based operation will be pursued by calculating the power required to be delivered to platform GFB (Eq. (1) to Eq. (3)). Afterwards, calculations for GFC are considered by following the flowchart (a) in Fig. 5. From GFC's operation, the power output of each GFC gas turbine is determined, as well as the value of power transfer between GFC and GFA. Lastly, the decision for the GFA platform's gas turbine power and the power allocated for the electrolyzer is determined according to the flowchart (b) in Fig. 5.

The flowcharts are strategically designed to adhere to economic efficiency rules. The number of gas turbines involved is determined by both the heat demand (N_{GTQ}) and the power demand (N_{GTP}). The electrical heater is utilized only if the gas turbines cannot meet the requirements adequately. Referring to diagram (a) in Fig. 5, GFC requests power from GFA only when all gas turbines are unable to fulfill the demands. Similarly, the same principles are applied to GFA (diagram (b) in Fig. 5), with an additional condition involving the electrolyzers' power, which is determined by comparing wind power to the aggregated demand on GFA.

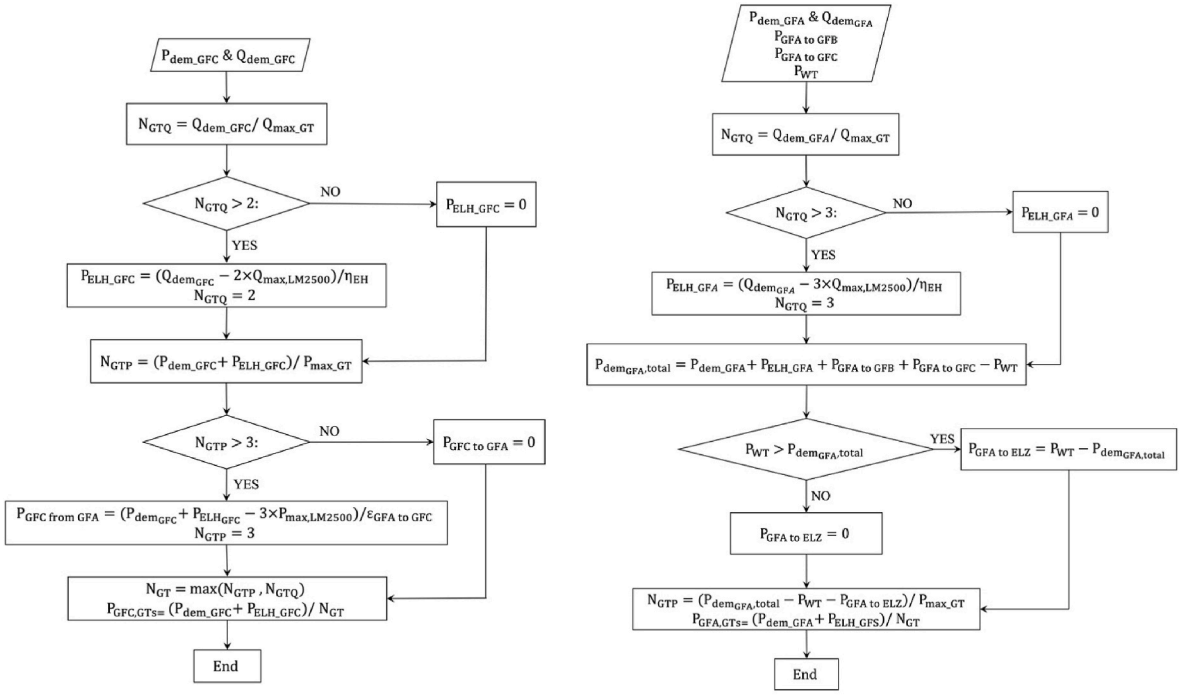

Fig. 5. Condition-based operation flowchart, (a) GFC operation, (b) GFA operation.

3.2. Scenario 2: optimization

While the condition-based operation excels in providing the best economically efficient decisions at each time step, leveraging optimization offers significant untapped potential in making energy management decisions over an extended time span. By incorporating an optimization code, the microgrid gains predictive capabilities, allowing it to anticipate future conditions, such as wind availability, and strategically plan its energy usage. For instance, the optimization code can intelligently choose to store excess energy during periods of high wind generation, ensuring a reserve for times when wind resources may be limited. This proactive approach optimizes energy storage and utilization, maximizing the utilization of renewable resources and minimizing reliance on conventional energy sources during adverse conditions. Consequently, the integration of predictive optimization empowers the microgrid to make well-informed, forward-looking decisions, resulting in enhanced overall performance and economic efficiency.

Another compelling advantage of the optimizer lies in its ability to manage the entire microgrid integration comprehensively. While the condition-based approach is confined to managing each platform separately according to predefined rules, the optimizer can holistically consider all assets, resources, and demands within the system. This increased freedom allows the optimizer to explore a wide range of possibilities and optimize the complex interplay of various components. However, this versatility also adds to the complexity of the optimization problem.

The optimization process involves testing numerous options and scenarios for running the microgrid over the given time span. Each scenario satisfies the energy balance requirements, but different costs and emissions are associated with each alternative. The iterative nature of the procedure enables the optimizer to continuously refine its approach, and ultimately identify the best solution that optimizes cost, efficiency, and emissions.

3.2.1. Digital twin of the microgrid

The optimizer relies on both precise predictions and high-speed processing to explore different scenarios effectively. To achieve this, the implementation of Artificial Intelligence (AI) techniques is essential in creating robust forecasting modules that anticipate changes in wind availability, demand patterns, and other dynamic factors. Moreover, the optimizer requires fast-responding models or "digital twins" of microgrid subsystems, and in the case of subsystems with nonlinear behavior, such as gas turbines and wind turbines, Artificial Neural Networks (ANNs) are utilized.

The use of ANN models allows for processing data, predicting system behavior, and capturing complex patterns through hidden layers, enabling accurate representations of the subsystems' dynamics. A Bayesian technique is utilized to tune the hyperparameters of the ANN models, employing Gaussian process models (Wu et al., 2019). The training of ANNs for gas turbines and wind turbines is conducted using the backpropagation algorithm, with 80% of the data allocated for cross-validation and the remaining 20% for testing. Detailed information on the hyperparameters and models' inputs and outputs can be found in Table 2 and Table 3, respectively. Additionally, for the electrolyzer, a polynomial regression is applied to fit the efficiency curve shown in Fig. 3, while the hydrogen flow rate is calculated using Eq. (12).

Table 2
Subsystem models inputs and output.

Subsystem	Input parameters	Output parameters
Gas turbine	$P_{MGT,dem}, FR, T_{amb}$	$\dot{m}_f$
Wind turbine	$T_{amb}, p_{amb}, S_W, D_W$	P_{WT}
Electrolyzer	P_{ELZ}	$\dot{m}_{H_2}$

$$\dot{m}_{H_2} = \eta_{ELZ} \times \frac{P_{ELZ}}{LHV_{H_2}} \tag{12}$$

The gas turbine models used in this study were developed based on real data, obtained from operating the LM2500 gas turbine with natural gas on an offshore platform. To create a model capable of predicting gas turbine operation with blends of natural gas and hydrogen, the models were fine-tuned and adjusted slightly using insights from the results presented in (Stuen, 2021), which investigated the impact of hydrogen fuel on LM2500 engines.

The accuracy of the models is evaluated by calculating maximum absolute error (mAE), mean absolute error (MAE), and mean absolute percentage error (MAPE) as defined in Eqs. (13) and (14). In the equations, X_{act} and X_{pred} are the actual values and predicted values from the model and n is the number of data in the test set. The errors are reported in Table 4.

$$MAE = \frac{1}{n}\sum_{i=1}^{n}\left|X_{pred} - X_{act}\right| \tag{13}$$

$$MAPE = \frac{1}{n}\sum_{i=1}^{n}\left|\frac{X_{pred} - X_{act}}{X_{act}}\right| \tag{14}$$

The gas turbine and wind turbine's model prediction in comparison to real operation data is visualized in Fig. 6. The model takes into careful consideration the NOx emissions of the gas turbines.

3.3. Optimization parameters and objective function

In addressing the current challenge, the optimization process must accomplish multiple tasks, including identifying power set-points for all gas turbines, determining the hydrogen/natural gas blend for GFA-GT1, and deciding on the power input to the electrolyzer. To optimize the microgrid's operation, a day of operation is considered to be the optimization window, and the smart management system must conduct the optimization ahead of this time span. The management system operates at a time step of 1 h, necessitating it to make decisions for the dispatchable units (gas turbines and electrolyzer) every hour, summing up to a total of 216 parameters (9 × 24 h). These parameters must be carefully established to optimize the microgrid's performance. Each parameter is bound by defined upper and lower limits based on its specific physical characteristics.

The gas turbines' power setpoint is constrained within the range of 9–22 MW, as defined in Eq. (15). Additionally, the hydrogen/natural gas blend for the GFA-GT1 engine is subject to a limitation, considering that the LM2500 gas turbine can tolerate a maximum hydrogen volume of 75%. These bounds are incorporated into the model through the fuel heating value ratio (FHR), defined in Eq. (16). With a lower heating value of 12.7 MJ/m^3 for hydrogen and 40.6 MJ/m^3 for methane, the engine's acceptable minimum FHR is determined to be 0.516 (Eq. (17)). Furthermore, the power allocated to the electrolyzer is restricted by its capacity to ensure it does not exceed its operational limit (90 MW), as outlined in Eq. (18).

$$P_{GT} = \left[P_{GT,1}, P_{GT,2}, \ldots, P_{GT,24}\right], P_{GT,min} < P_{GT,i} < P_{GT,max} \tag{15}$$

$$FHR_{GT} = (\dot{m}_{NG} \times LHV_{NG}) / (\dot{m}_{NG} \times LHV_{NG} + \dot{m}_{H_2} \times LHV_{H_2}) \tag{16}$$

$$FHR_{GT} = \left[FHR_{GT,1}, FHR_{GT,2}, \ldots, FHR_{GT,24}\right], 0.516 < FHR_{GT,i} < 1 \tag{17}$$

$$P_{GFA\_to\_ELZ} = \left[P_{GFA_{to_{ELZ,1}}}, P_{GFA_{to_{ELZ,2}}}, \ldots, P_{GFA_{to_{ELZ,24}}}\right], 0 < P_{GFA\_to\_ELZ,i} < P_{GFA\_to\_ELZ,max} \tag{18}$$

The primary objective of the optimization process is to minimize the total cost of operation, which encompasses various factors (Eq. (19)). These factors include the cost of purchasing natural gas (C_{NG}), the taxes

Table 3
ANN models optimized configuration.

Subsystem	No. of neurons, layer 1	No. of neurons, layer 2	No. of neurons, layer 3	AF, layer 1	AF, layer 2	AF, layer 3	LR
Gas turbine	42	17	–	sigmoid	ReLU	–	0.72
Wind turbine	45	100	22	SELU	ReLU	linear	0.57

Table 4
Models prediction error.

Subsystem	mAE	MAE	MAPE
Gas turbine	0.017 [kg/s]	0.004 [kg/s]	0.21%
Wind turbine	0.801 [MW]	0.152 [MW]	0.61%
Electrolyzer	1.6e-5 [kg/s]	1.2e-5 [kg/s]	0.05%

associated with CO_2 and NOx emissions ($C_{NG,tax}$ and $C_{NOx,tax}$), as well as the maintenance costs related to the gas turbines and electrolyzation components (C_{MGT} and C_{ELZ}).

$$C_{total} = C_{NG} + C_{NG,tax} + C_{NOx,tax} + C_{MGT} + C_{ELZ} \quad (19)$$

The first two terms of the total cost equation (Eq. (19)) are determined based on the total amount of natural gas consumed by all 7 gas turbines throughout the optimization day. The cost of purchasing natural gas (C_{NG}) is calculated using the daily fuel price. The term $C_{NG,tax}$ represents the specific tax imposed by the Norwegian government on natural gas to regulate CO_2 emissions. For the petroleum industry, the tax value in 2022 amounted to 1.65 NOK (about 0.16 EUR) per standard cubic meter of natural gas consumed ("Tax rates in Norway).

The tax for NOx emissions ($C_{NOx,tax}$) is computed based on the NOx emitted from the engines, which is calculated using the power output of each engine at each time step. A correlation between NOx emissions and power output is established, fitted to real data presented in Fig. 7, derived from measurements obtained from the actual engine and reported in (Sundsbø Alne, 2007). The value of tax for NOx emissions was 23.79 NOK (about 2.36 EUR) per kilogram of emission in 2022 ("Tax rates in Norway). Additionally, the maintenance cost of the gas turbines, electrolyzer, compressor, and water desalination system is computed using the values reported in (Tilocca et al., 2023).

The optimization process primarily aims to reduce the calculated cost, but an additional factor must be considered in the objective function and that is the preservation of hydrogen in the tank. Focusing solely on cost reduction would lead the optimization algorithm to prioritize immediate hydrogen consumption, disregarding its potential future value when wind power is limited. To address this issue, it becomes crucial to incentivize the preservation of hydrogen at the end of each day.

Optimizing for a limited time span means that the optimizer's vision is confined to that specific window, and it cannot anticipate future needs beyond that period. Consequently, it may use the stored hydrogen at early time steps, potentially missing the opportunity to benefit from it in subsequent optimization windows. To counteract this, it is essential to encourage the preservation of hydrogen for future utilization.

This incentive is essential irrespective of the optimization window's duration, as it accounts for an unpredictable future following any finite period of optimization. To calculate this incentive, an estimation of the saved hydrogen's value for the next day is necessary, as it can offset natural gas costs, including both price and tax. The incentive for preserving hydrogen is determined using Eq. (20).

$$Inc_{HyT} = m_{HyT} \times \frac{LHV_{H_2}}{LHV_{NG}} \times \left(C_{NG} + C_{NG,tax}\right) \quad (20)$$

Consequently, the objective value to be reduced by the optimizer will become as stated in Eq. (21):

$$OV = C_{total} - Inc_{HyT} \quad (21)$$

3.3.1. Hybrid optimization approach

Optimizing the power setpoints for each gas turbine and the electrolyzer can lead to significantly long computational times due to a large number of optimization parameters (9 × 24 parameters for each day). Additionally, the consideration of constraints (Eq. (1) to Eq. (11)) further adds to the duration of optimization. Notably, the hydrogen fuel conservation constraint (Eq. (11)) introduces complexity to the problem due to its nature.

This constraint ensures that the hydrogen consumption at each time step "i" (dependent on $P_{GFA-GT1,i}$ and FHR_i) must not exceed the amount available in the tank. However, the tank's content is influenced by both the hydrogen produced (dependent on $P_{GFA-to-ELZ}$)) up to that time step and the hydrogen consumed (dependent on $P_{GFA-GT1}$ and FHR) up to

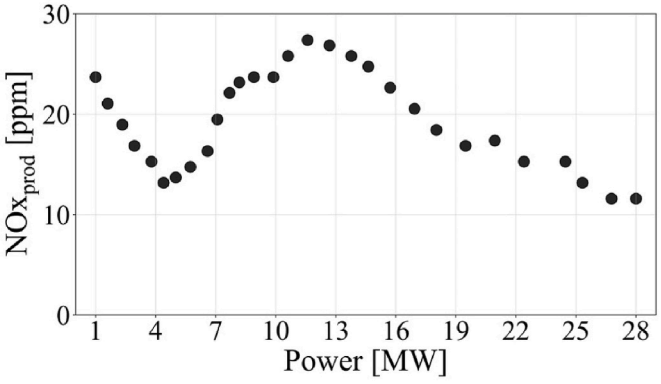

Fig. 7. NOx production at different power outputs of LM2500 (Sundsbø Alne, 2007).

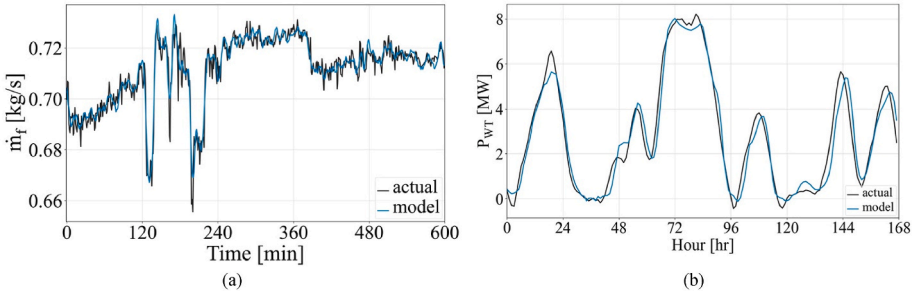

Fig. 6. Visualization of ANN models' accuracy, (a) gas turbine, (b) wind turbine.

that time step. These quantities are also optimization parameters, making the constraint interrelated with the optimization parameters, resulting in intricacies within the optimization process. The constraint is shown in Eq. (22) below:

for $1 \leq i \leq 24$:

$$\psi\left(FHR_1, FHR_2, \ldots, FHR_i, P_{GFA-GT1,1}, P_{GFA-GT1,2}, \ldots, P_{GFA-GT1,i}, P_{GFA-to-ELZ,1}, P_{GFA-to-ELZ,2}, \ldots, P_{GFA-to-ELZ,i-1}\right) \leq 0 \quad (22)$$

To overcome the complications of the optimization, a novel hybrid approach is proposed to enhance the optimization process while ensuring compliance with constraints. The approach involves prioritizing the optimization of power balance for each platform, rather than focusing solely on optimizing individual components such as gas turbines and the electrolyzer. The optimizer first determines the most favorable power transfer values between GFA and GFC, as well as between GFA and ELZ, to achieve an optimized power balance across the system. Subsequently, the optimal operation of gas turbines on each platform is determined in the next step. This decision for each platform is based on the power balance requirements derived from the platform's demand and the power transfers identified in the preceding step.

Therefore, the optimization algorithm is structured into two levels: the field optimization level (outer optimization loop) and the platform optimization level (inner loop). At the field optimization level, the focus is on searching for the optimum power transfer values. Once these values are set, the platform optimization level takes over to optimize the operation of the gas turbines based on the power balance requirements.

By breaking down the optimization process into two levels, the number of optimization parameters is reduced. This reduction mitigates the challenges associated with the curse of dimensionality. Additionally, the constraints of power balance are imposed between the two optimization levels, ensuring a stable and reliable system operation.

The outer loop optimization, which plays a critical role in the process, utilizes Genetic Algorithm (GA) for efficient decision-making. For platform optimization (the inner loop), a simplified approach is employed to reduce computational costs. Prior to optimization, a comprehensive database of platform operations is prepared, encompassing all possible combinations of engine operation within the platform. The platform optimizer's task is to search through this database and identify combinations that meet the power and heat demand requirements. From these combinations, the optimizer selects the one with the lowest cost among the available choices. The optimization process flowchart is depicted in Fig. 8, providing an overview of the optimizer's operation. As it is depicted, within the GA optimization loop, the optimizer determines the power flow of transmission cables and the fuel heating value ratio of GT1 on GFA.

In the next step, the net power imposed on each platform is calculated based on the demand of the platform and the transferred values defined by the level 1 optimizer. Subsequently, the optimization of platforms A and C is carried out based on the net power and heat demand of the platform. The optimizer selects rows from the database that closely align with the boundary conditions for heat and power output. From these rows, the optimizer chooses the solution with the minimum cost.

The proposed hybrid optimization approach results in a much faster optimization process. The platform optimization (inner loop, level 2) is a table look-up and filtering process, which consumes minimal time. Most of the optimization duration is attributed to field optimization, which involves only 72 (3×24) parameters. By reducing the number of optimizing parameters, the method significantly increases the speed of optimization. Within just 1 h of running the optimization, the proposed approach provides the optimized answer. This reduction in computational time allows for more rapid decision-making and real-time adjustments to achieve optimal power balance and platform operations in the offshore microgrid.

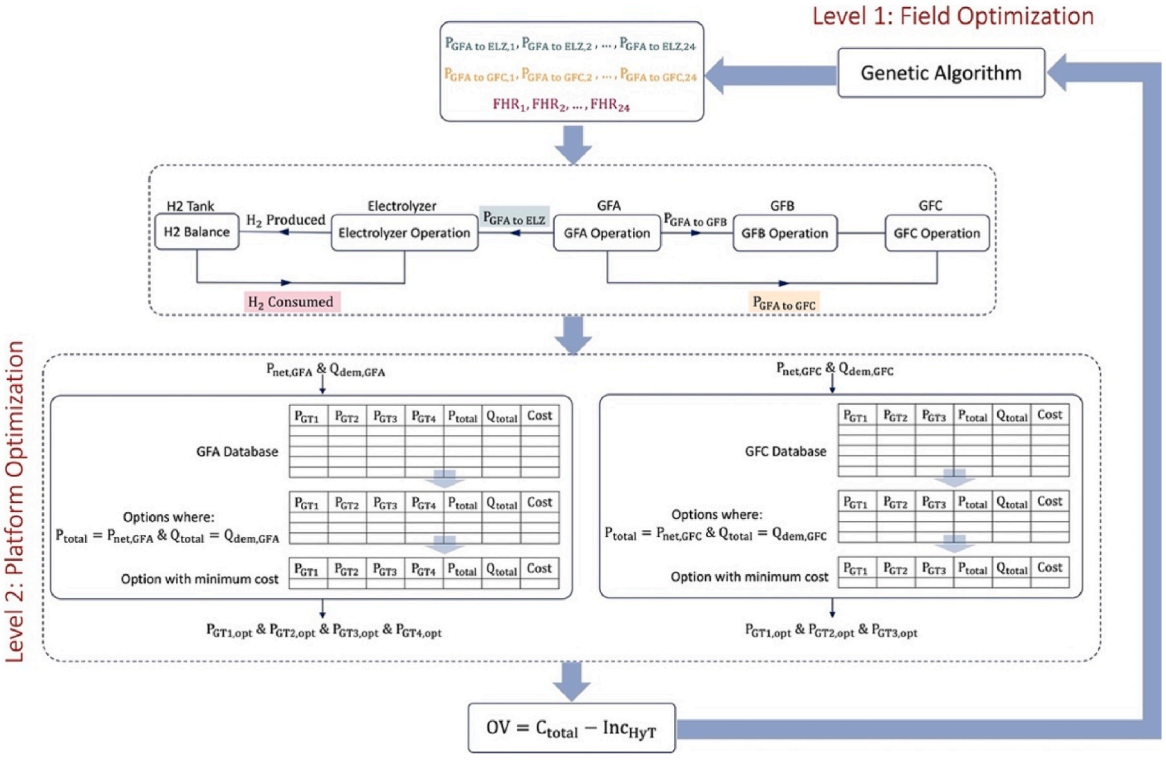

Fig. 8. The new optimization approach; the outer loop is responsible for power flow in connection cables and fuel ratio, and the inner loop optimizes the platforms' operation.

4. Results and discussion

The integrated microgrid of Gullfaks field and Hywind Tampen, along with the electrolyzer, is simulated to evaluate its operation for a week-long period from 24/01/2022 to 30/01/2022. The simulation includes both condition-based and optimization approaches to assess the benefits of employing an optimizer in the process. While the condition-based approach provides immediate decisions for each time step during operation, the optimizer requires pre-planning and provides decisions in advance within a designated optimization window. In this study, the optimization window spans a day, and the time step is set at 1 h, allowing for hourly variations in operational decisions.

The utilization of the optimizer necessitates the use of forecast data instead of actual data prior to the operation. Weather data plays a critical role in estimating the power output from wind farms and serves as an input for the gas turbine model. In this study, weather forecasts were obtained from the Norwegian Meteorological Institute (Norwegian Meteorological Institute, 2022), which provides updates every 6 h. Specifically, the forecast data utilized in this research was collected from the 6 p.m. update the day before. Both the forecast data employed for optimization and the actual weather data used in the condition-based operation are depicted in Fig. 9. Fig. 10 illustrates the wind power calculated by the wind turbine model based on both the actual weather data and the forecasted data.

To optimize the microgrid, accurate knowledge of the platforms' demand patterns is crucial. However, due to the unavailability of detailed demand data and historical records for the Gullfaks platforms, only average values and common variations are accessible (Tangerås and Tveiten, 2018). As a result, constructing a demand model and providing precise forecasts based on historical data and weather information becomes infeasible. Nevertheless, previous studies in demand prediction have shown promising results, achieving a mean absolute error of less than 5% (Tan et al., 2019). In this study, the demand patterns are generated based on the available information from (Tangerås and Tveiten, 2018), utilizing random distributions. Fig. 11 presents the demand profiles for the three platforms. The power demand distribution is generated using a random distribution, incorporating specific values for the average, minimum, and maximum values collected from (Tangerås and Tveiten, 2018). A similar approach is applied for the heat distribution, but with a sequential pattern that aligns more closely with the platform's heating demands. The criteria employed for demand data generation are reported in Table 5.

The forecasted demand is adjusted using randomly distributed error values, with a maximum deviation of 7% and a mean of 5%. It is important to note that the literature suggests achieving demand predictions with a maximum error of 5% for O&G platforms (Tan et al., 2019). However, in this work, a deliberately higher error margin is considered to ensure a conservative approach.

Over the course of the week, the combined power demand from the three platforms amounts to 59,203 GJ, while the total heat demand is 11,969 GJ. The power generated by the wind farm during this period is 55,373 GJ, resulting in a shortfall of 3830 GJ to meet the power demand or 15,799 GJ when considering both heat and power requirements. The deviation of wind power from the total power demand is visualized in Fig. 12. Notably, there are three distinct time periods with low wind power generation, indicating a need for increased participation of gas turbines in the operation during those intervals. For the remaining duration of the week, the wind power aligns relatively closely with the total power demand, although occasional surpluses and deficiencies are observed.

The simulation started with an empty hydrogen tank at the beginning of the week. In the condition-based approach, each time step (1 h) throughout the week was analyzed hence the flowcharts shown in Fig. 5 were conducted 7×24 times. The optimization process, on the other hand, was run seven times, with each run taking approximately 1 h to complete. The condition-based operation was carried out using actual data at each hour, while the optimizer was employed one day ahead of the actual day of operation, utilizing forecasted data. A visual comparison of these two approaches is provided in Fig. 13.

It is important to highlight that although the optimizer in this study utilized forecast data to conduct the optimization process, the evaluation of its performance is conducted based on real data to mirror real-life applications. In practical use, the optimizer relies on forecasts to generate an efficient schedule, but its true value lies in how well this schedule performs on the actual day when the real wind power or demands arises. Therefore, accurate forecasts and models are crucial to achieve optimal performance from the optimizer. Otherwise, the deviation between forecasted and real data may significantly impact the optimizer's efficiency. In the current study, the optimized schedule resulted in low costs, which slightly increased when real values were employed on real data which was due to forecast errors when compared to actual data.

The total power generated by all the gas turbines is presented in Fig. 14. As depicted, the optimizer successfully managed to operate the gas turbines with considerably less power compared to the condition-based approach. However, there were three time spans where the power production of the gas turbines was nearly the same for both scenarios. These time spans coincided with periods of wind power deficiencies (Fig. 12).

Figs. 15 and 16 provide the total power produced by each platform. The analysis of Figs. 15 and 16 highlights interesting observations regarding the gas turbine performance in the optimized and condition-based scenarios. Notably, GFA demonstrates slightly higher power output from the gas turbines in the optimized scenario compared to the condition-based scenario, while the opposite trend is observed for GFC.

In both scenarios, the gas turbine production in GFA remains below the total demand, primarily because wind power contributes to fulfilling a portion of the demand. This relationship is supported by the three

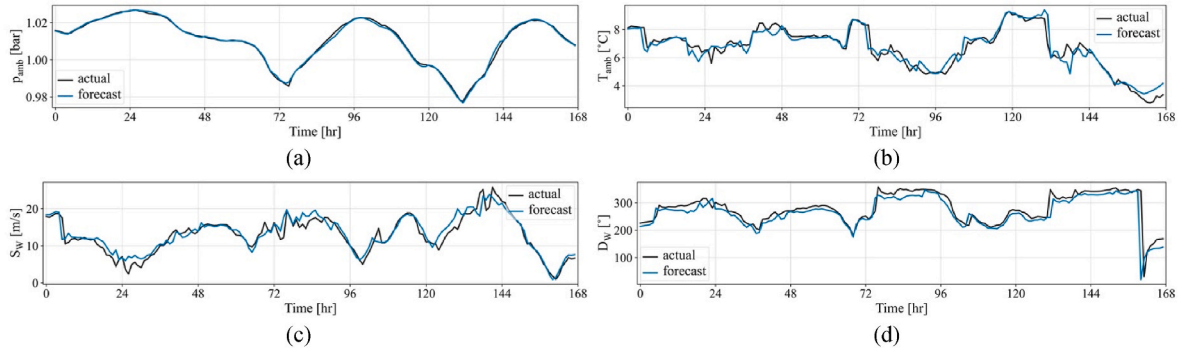

Fig. 9. Weather data and forecasts compared to real data, (a) ambient pressure, (b) ambient temperature, (c) wind speed, and (d) wind direction. The data is downloaded from (Norwegian Meteorological Institute, 2022).

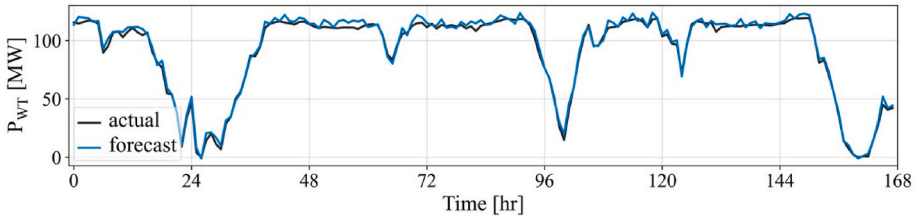

Fig. 10. Wind farm power production is calculated based on actual weather data as well as weather forecasts.

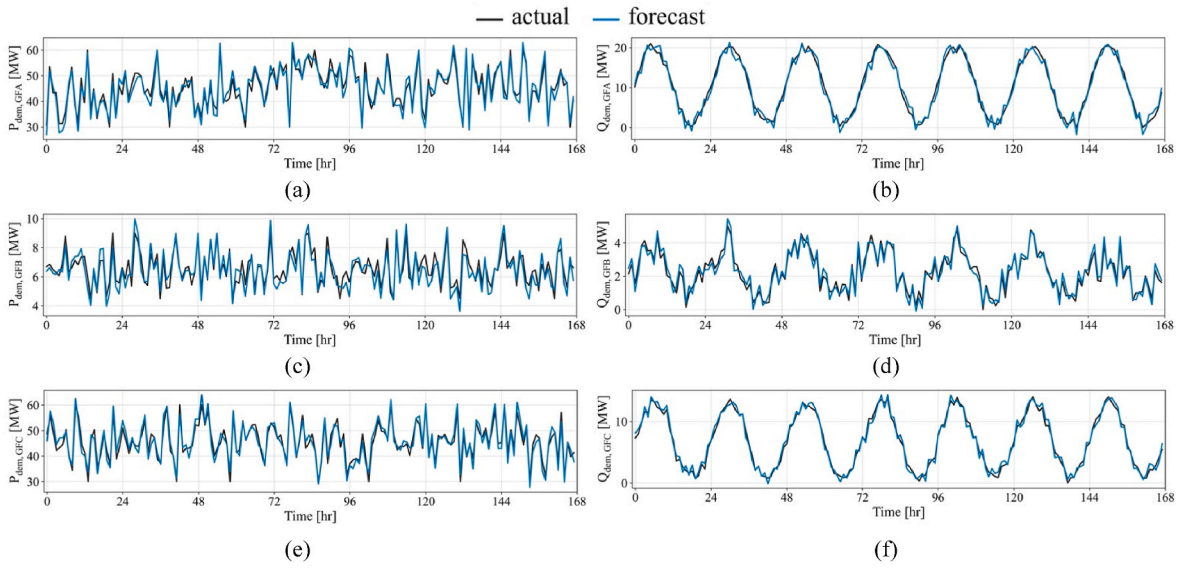

Fig. 11. Demand patterns and predictions for Gullfaks platforms, (a) demand power on GFA, (b) demand heat on GFA, (c) demand power on GFB, (d) demand heat on GFB, (e) demand power on GFC, and (f) demand heat on GFC.

Table 5
Models prediction error.

Platform	Power			Heat		
	max [MW]	mean [MW]	min [MW]	max [MW]	mean [MW]	min [MW]
GFA	60	36	30	21	15	0
GFB	9	5.4	4	5	2	0
GFC	60	36	30	14	10	0

instances of increased gas turbine production shown in Fig. 15, where the production of gas turbines reaches the demand values during periods of low wind power.

Conversely, in GFC, the gas turbines' production closely matches the demand in the condition-based scenario, but the optimized operation falls short of meeting the demand (Fig. 16). Examining Fig. 17 reveals that the optimizer opted to direct power from GFA to GFC in order to compensate for the shortfall. In other words, the optimizer decided to compensate for the GFC demand partly from its gas turbines, and partly by getting power from GFA. On GFA however, the power produced by gas turbines was more or less similar in the condition-based and optimization scenario. Therefore the power transmitted to GFC from GFA was not attributed to GFA gas turbines, but might be from the wind power. Fig. 17 can reveal the source of the power transmitted from GFA to GFC. This allocation pattern aligns with the variations in wind power, indicating that a portion of the wind power delivered to GFA is redirected to GFC in the optimized scenario. It could be seen that the power transmission from GFA to GFC during times of low wind power in the optimized scenario has been decreased in comparison to other times.

As mentioned earlier, power transmission between GFA and GFC is possible in both directions. The occurrences of power transfer from GFC to GFA seldom times, as indicated in Fig. 18, align with the times of deficiency in wind power production, which is expected.

Notably, for the condition-based operation, the power transmission option is used only if the gas turbines on the platform are incapable of meeting the demand (flowchart in Fig. 5), which is not the case in this study and therefore zero power transmissions for condition-based operation is shown in Figs. 17 and 18. However, the optimizer

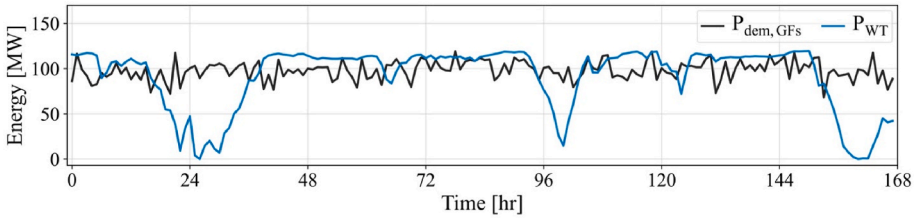

Fig. 12. Total power demand from three Gullfaks platforms vs. the power generated by the wind farm.

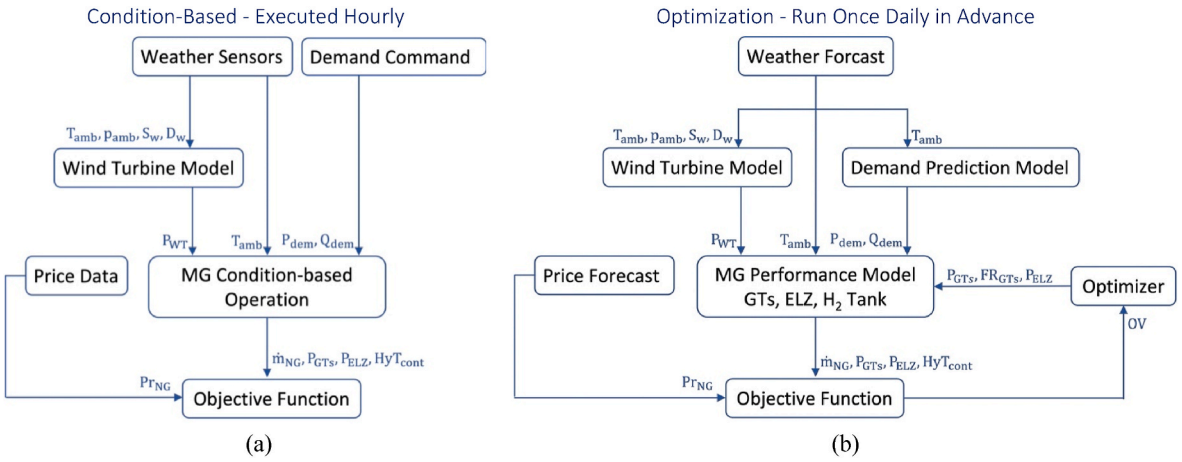

Fig. 13. The process of control and management of the microgrid and the data transfer; (a) condition-based and (b) optimization.

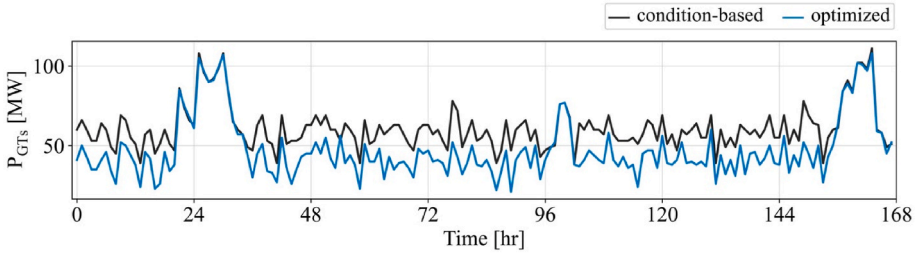

Fig. 14. The total power produced by the seven gas turbines on the three Gullfaks platforms.

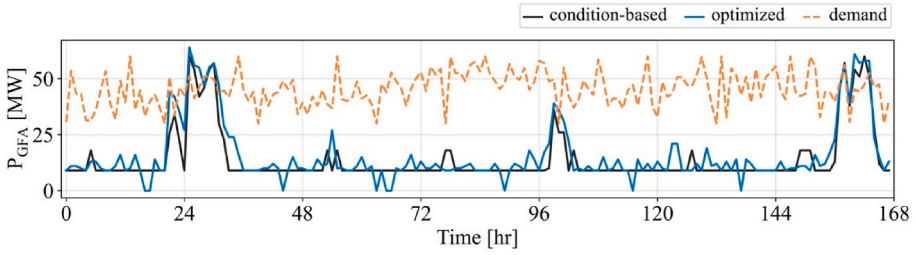

Fig. 15. The total power produced by the four gas turbines on the GFA platform.

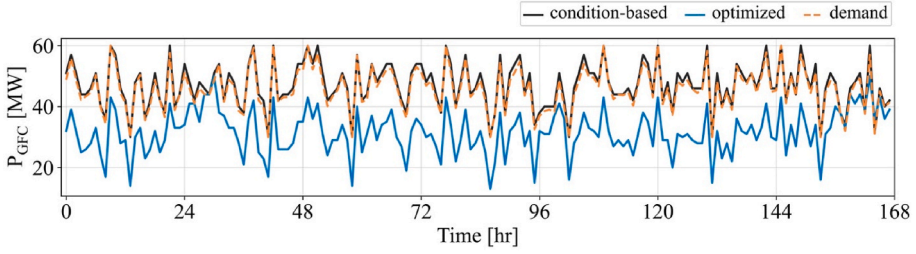

Fig. 16. The total power produced by the three gas turbines on the GFC platform.

discovers that it is more efficient to transfer power from other platforms rather than running the gas turbines on its own platform, as demonstrated in the optimized scenario in these figures.

In the optimized scenario, it was observed that the gas turbines produced less power compared to the condition-based operation. Instead, the optimized scenario utilized a greater proportion of wind power to meet the demands of the platforms. This naturally raises the question of what happens to the surplus power generated in the condition-based operation. The only plausible explanation is that it is stored through the allocation of power to water electrolysis and hydrogen production. The rates of hydrogen production and consumption for both scenarios are illustrated in Figs. 19 and 20, respectively, and the amount of hydrogen available in the tank is shown in Fig. 21. The data clearly indicates that the condition-based operation achieves greater energy savings, whereas the optimizer primarily utilizes energy during the optimization window.

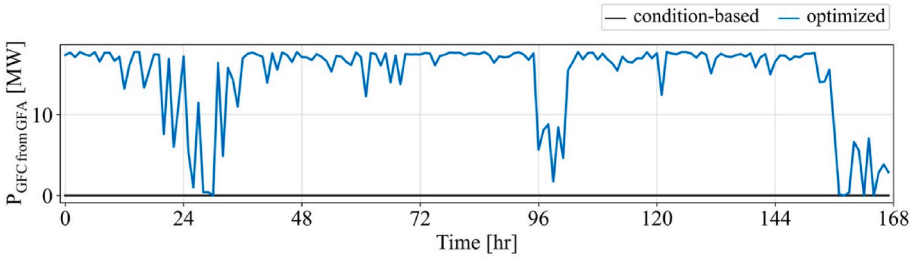

Fig. 17. The power received by GFC from GFA.

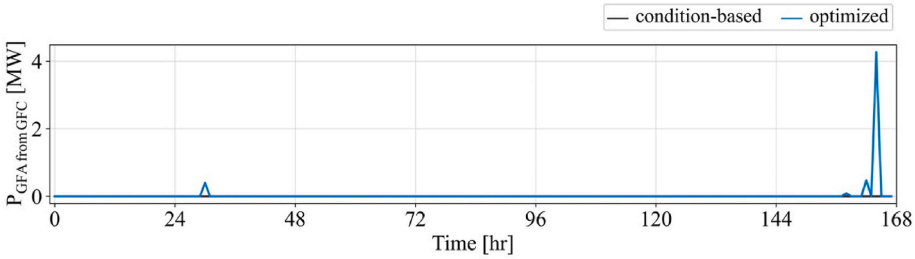

Fig. 18. The power received by GFA from GFC.

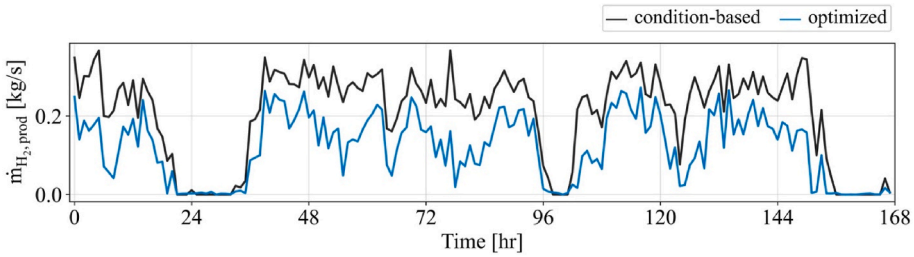

Fig. 19. The rate of hydrogen production.

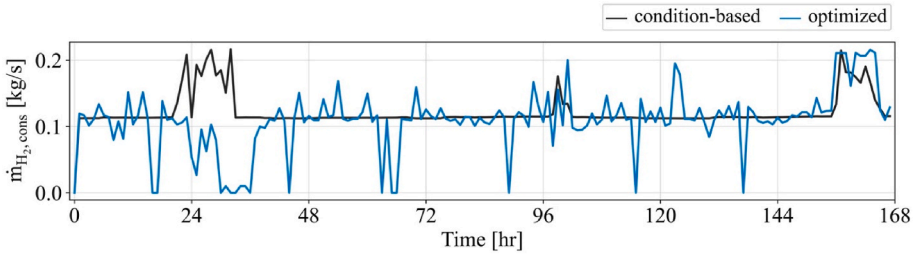

Fig. 20. The rate of hydrogen consumption.

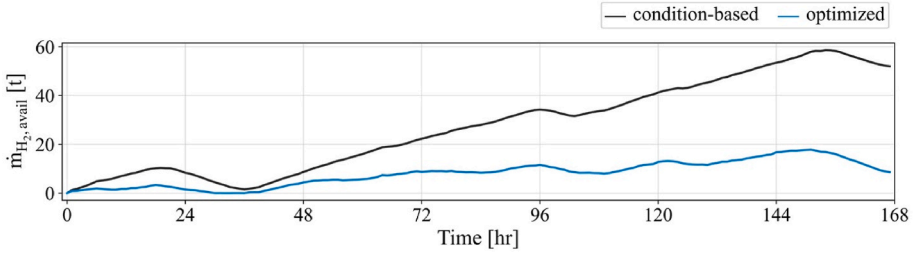

Fig. 21. Hydrogen fuel availability over the week.

Examining the consumption pattern in Fig. 20 reveals distinct differences between the condition-based and optimized operations. The condition-based scenario exhibits a consistent pattern of hydrogen consumption, with mostly constant values, but higher consumption during periods of wind deficiency. On the contrary, the optimized scenario shows more variability in hydrogen usage. Understanding the optimizer's decision-making process for hydrogen usage is challenging, as it depends not only on the tank's available quantity but also considers its impact on the cost of the current and subsequent optimization windows, as previously discussed and implemented through the hydrogen saving incentive (Eq. (20)). Never the less, it is evident from Fig. 21 that the rate of filling the hydrogen tank in condition-based operation is considerably higher than the optimization.

An overview of the total hydrogen balance for both scenarios is presented in Table 6. The relative difference reported in the tables is calculated according to Eq. (23).

$$X_{\text{rel diff}} = \left(X_{\text{optimized}} - X_{\text{condition}-\text{based}}\right) / X_{\text{condition}-\text{based}} \times 100 \quad (23)$$

Although conducting a direct hourly comparison between the condition-based operation and the optimized scenario is complex, certain observations have become evident. The condition-based approach prioritizes saving more energy and transferring less between platforms, while the optimized scenario takes the opposite approach. It should be noted, as depicted in Fig. 3, that the maximum energy-saving efficiency cannot exceed 70%. However, when power is transmitted between GFA and GFC, only 11% of the energy is wasted. Consequently, the optimizer takes advantage of this option and efficiently manages the platforms through an integrated approach. In contrast, the condition-based operation adopts a more localized approach, with power transmission between platforms occurring only when necessary. An overview of the costs, emissions, and fuel consumption for both scenarios is reported in Table 7.

The optimizer's operation throughout the week exhibits a cost reduction of 16.32% compared to the condition-based approach. However, it is important to consider the impact of the disparity in the amount of hydrogen remaining in the tank. After all, the hydrogen in the tank is a source of power that will not entail the costs associated with natural gas (C_{NG} and $C_{NG,tax}$ in Eq. (19)). To assess this, the cost savings attributed to the hydrogen quantity are calculated by comparing the costs of using natural gas with an equivalent heat value, as detailed in Table 7 under the column "H_2 res. cost red.". The findings reveal that despite the condition-based scenario having a higher quantity of saved hydrogen in the tank, the optimizer still manages to achieve approximately a 12.44% cost reduction. It should be noted that the gap in hydrogen availability rates will eventually stabilize once the tank reaches full capacity. At that point, it is expected that the optimizer will consume less hydrogen, as observed during this case study. Consequently, the cost reduction prospects will continue to favor the optimized operation.

The optimized operation demonstrates a notable decrease of 16.42% in the total consumption of natural gas compared to the condition-based approach, reflecting a similar relative difference in carbon-based emissions. However, it is important to note that the optimized operation experienced a slight increase of 0.9% in NOx emissions compared to the condition-based operation. This outcome can be attributed to the gas turbine's high NOx emissions at low power outputs, as illustrated in Fig. 7. Despite the optimized operation's reduced reliance on gas turbines, the emission levels were slightly higher.

Table 6
Comparison of hydrogen balance after a week of operation by different scenarios.

	H2 prod.	H2 cons.	H2 res.
Condition-based	124.98 [t]	73.40 [kg]	51.58 [t]
Optimized	72.89 [t]	65.79 [kg]	7.10 [t]
Relative difference	−41.68%	−10.37%	−86.23%

Table 7
Overview of cost balance after a week of operation by different scenarios.

	NG cons.	NOx prod.	Total Cost	H2 res. cost red.	Total Cost - mod
Condition-based	2684.30 [t]	4.40 [t]	1136109 [€]	59657 [€]	1076452 [€]
Optimized	2243.65 [t]	4.44 [t]	950741 [€]	8213 [€]	942529 [€]
Relative difference	−16.42%	0.90%	−16.32%	−86.23%	−12.44%

It is worth mentioning that the objective function solely focuses on operational costs (as shown in Eq. (19)). Therefore, the motivation to reduce NOx emissions primarily stems from the NOx tax. If there is a greater emphasis on minimizing NOx emissions, one can introduce an increasing coefficient (a value greater than 1) before the term $C_{NOx,tax}$ in Eq. (19) to guide the optimizer towards more effective NOx reduction strategies.

The optimization operations discussed in this paper were primarily conducted within a 24-h window. However, the authors also explored the effects of shorter and longer optimization windows, yielding similar results. Interestingly, as the optimization window lengthened, the performance of the optimization process exhibited only marginal improvements. Nevertheless, extending the optimization window significantly increased the duration of the optimization process due to the larger number of parameters to optimize.

One advantage of utilizing a shorter optimization window is the enhanced accuracy of weather and demand data forecasts. For instance, if a 6-h window is employed, the optimizer can utilize more precise weather forecast values during the final hours of the same day. In contrast, a 24-h window necessitates relying on weather forecast values from the following day. Similar improvements in accuracy can be observed in demand forecasts when shorter prediction periods are utilized. However, it should be noted that as the optimization window decreases in duration, the performance of the optimizer diminishes. For example, in the examined 6-h version, the relative total cost reduction was −16.27% (instead of 16.32%). Thus, a trade-off between the optimizer's performance and the duration of optimization must be carefully considered.

5. Conclusion

This work introduced an integrated energy management system for an offshore microgrid comprising three petroleum platforms, a floating wind farm, and a setup for green hydrogen production and storage. Two of the platforms housed seven aero-derivative gas turbines, providing power and heat. A management tool was developed by integrating highly accurate, fast-response models of all components, representing a digital twin of the system. Actual component data were utilized with an AI approach to develop the digital twin. The study explored two operation approaches: "condition-based" with predefined economic rules for demand and production balance, and "optimization" which forecasted demands and renewable production to determine the efficient, low-cost, and low-emission solution.

The study presented a novel hybrid optimization approach for enhancing energy management efficiency. The algorithm involved two levels: field optimization with Genetic Algorithm, and platform optimization using a rapid database searching process. This approach achieved optimized solutions within 1 h, enabling real-time adjustments and fast decision-making in the offshore microgrid.

The research demonstrated that the intelligent management system, i.e., the optimizer operation, significantly enhances overall performance, compared to the already economical condition-based approach. Over a week of operation, the optimized scenario resulted in a 16% of cost reduction (c.a. 185,000 €) and a 16% reduction in natural gas

consumption and carbon-based emissions. The study's optimized scenario effectively determined the best operation schedule by considering the entire field and integrating units' operations. This success resulted from overcoming the limitations of the condition-based approach, which relied on a "platform approach" and predefined rules, lacking the ability to fully utilize all microgrid assets. In contrast, the optimization problem's complexity necessitated exploring different combinations of assets' operations to achieve cost efficiency; a task accomplished using demand and production forecasts.

The significance of this work can be summarized as follows:

- The study provided a real case study of an offshore petroleum field with minimal simplification, moving beyond conceptual microgrids typically studied in related literature and presenting a more realistic assessment with complex power connections between platforms.
- Unlike many microgrid studies, this work considered demand balance with respect to both power and heat. The inclusion of gas turbines equipped with waste heat recovery units enabled the management systems (condition-based and optimized) to address heat balance efficiently and also enhanced the realism of the study.
- The introduction of a hybrid optimization approach, utilizing both genetic algorithms and a database search, significantly reduced the computational time required for microgrid optimization. This allowed for the optimization of a day's operation within hourly schedules for all microgrid units.
- The use of the Python language and execution on a standard personal laptop underscored the efficiency and scalability of the proposed hybrid optimization method. This makes the approach practical and accessible for real-world offshore microgrid systems without the need for extensive computing resources.

While the advantages of the introduced method are highlighted, a few points must be considered:

- Model accuracy is crucial for the system's performance. Since all of the models are data-driven, access to operational data from the gas turbines, wind turbines, and electrolyzer is essential for developing highly accurate models.
- Data access readiness over time is also important for maintaining model accuracy as the microgrid components age. Periodic retraining of models with new data ensures the maintaining accuracy of the models.
- The accuracy of the demand forecast model is dependent on the quality and reliability of the weather forecasts, which are provided by meteorological institutions. It is essential to carefully select a trustworthy source of weather forecasts to ensure the performance of the developed structure.
- The two-level optimization approach improves efficiency but has limitations. Optimal results depend on database quality and the genetic algorithm's exploration of the outer loop. Enhancements in microgrid performance are possible with improved complexity and database accuracy.

In conclusion, this study introduced a smart integrated microgrid management system with low development costs, achieving significant cost and emission reduction in petroleum operations. These findings contribute to a more sustainable energy future in the offshore O&G industry, emphasizing the potential of advanced energy management techniques in addressing climate change and promoting environmental responsibility.

CRediT authorship contribution statement

Reyhaneh Banihabib: Conceptualization, Methodology, Data curation, Software, Development, Writing – original draft, Writing – review & editing. **Mohsen Assadi:** Funding acquisition, Supervision.

Declaration of competing interest

The authors declare the following financial interests/personal relationships which may be considered as potential competing interests: Reyhaneh Banihabib reports financial support was provided by European Union's Horizon 2020 research and innovation program under the Marie Skłodowska-Curie grant agreement No. 861079.

Data availability

The data will be uploaded alongside the article

Acknowledgments

This project has received funding from the European Union's Horizon 2020 research and innovation program under the Marie Skłodowska-Curie grant agreement No. 861079. The authors wish to acknowledge Dr. Arild N. Nystad for his valuable input and support during the formative stages of this research, which greatly contributed to the development of the ideas presented in this paper.

Nomenclature

AI	Artificial Intelligence
ANN	Artificial Neural Network
C	Cost
dem	Demand
ELZ	Electrolyzer
ETS	European Union Trading System
FHR	Fuel heating value ratio
GFA	Gullfaks A
GFB	Gullfaks B
GFC	Gullfaks C
GHG	Greenhouse gases
GT	Gas turbine
hr	Hour
HyT	Hydrogen tank
IEM	Integrated energy microgrids
Inc	Incentive
LHV	Lower heating value
LNG	Liquefied Natural Gas
M	Mass (stored)
m	Mass (consumption)
MAE	Mean absolute error
MAPE	Mean absolute percentage error
NCS	Norwegian Continental Shelf
O&G	Oil and gas
ov	Objective value
P	Power
N	Number of gas turbines
NG	Natural gas
Q	Heat
red	Reduction
res	Reserved
R&D	Research and Development
WHRU	Waste heat recovery unit

References

LM2500 & LM2500XPRESS Gas Turbines | GE Gas Power." https://www.ge.com/gas-power/products/gas-turbines/lm2500 (accessed May 25, 2023).

Adrian, Hjellestad, 2022. Offshore Wind Power and Hydrogen for Oil and Gas Platform Electrification. Masters, University of Bergen, Bergen, Norway.

Al-Shetwi, A.Q., 2022. Sustainable development of renewable energy integrated power sector: trends, environmental impacts, and recent challenges. Sci. Total Environ. 822, 153645 https://doi.org/10.1016/j.scitotenv.2022.153645.

Amin, K., Fors, T., 2020. Hydrogen Power with Siemens Gas Turbines.

Anekwe, I.M.S., Tetteh, E.K., Akpasi, S., Atuman, S.J., Armah, E.K., Isa, Y.M., 2023. Carbon dioxide capture and sequestration technologies – current perspective, challenges and prospects. In: Green Sustainable Process for Chemical and Environmental Engineering and Science. Elsevier, pp. 481–516. https://doi.org/10.1016/B978-0-323-99429-3.00034-5.

Anglani, N., Di Salvo, S.R., Oriti, G., Julian, A.L., 2020. Renewable energy sources and storage integration in offshore microgrids. In: 2020 IEEE International Conference on Environment and Electrical Engineering and 2020 IEEE Industrial and Commercial Power Systems Europe (EEEIC/I&CPS Europe). IEEE, pp. 1–6. https://doi.org/10.1109/EEEIC/ICPSEurope49358.2020.9160760.

Brenntrø, J., 2016. Process Simulation and Evaluation of Options for Heat and Power Generation on Offshore Oil and Gas Installations. Norwegian University of Science and Technology, Trondheim.

Cheng, C., Hughes, L., 2023. The role for offshore wind power in renewable hydrogen production in Australia. J. Clean. Prod. 391, 136223 https://doi.org/10.1016/j.jclepro.2023.136223.

de Souza Nascimento, M.M., Shadman, M., Silva, C., de Freitas Assad, L.P., Estefen, S.F., Landau, L., 2022. Offshore wind and solar complementarity in Brazil: a theoretical and technical potential assessment. Energy Convers. Manag. 270, 116194 https://doi.org/10.1016/j.enconman.2022.116194.

Desmond, C., Murphy, J., Blonk, L., Haans, W., 2016. Description of an 8 MW reference wind turbine. J Phys Conf Ser 753, 092013. https://doi.org/10.1088/1742-6596/753/9/092013.

Dokhani, S., Assadi, M., Pollet, B.G., 2023. Techno-economic assessment of hydrogen production from seawater. Int. J. Hydrogen Energy 48 (26), 9592–9608. https://doi.org/10.1016/j.ijhydene.2022.11.200.

Durakovic, G., del Granado, P.C., Tomasgard, A., 2023. Powering Europe with North Sea offshore wind: the impact of hydrogen investments on grid infrastructure and power prices. Energy 263, 125654. https://doi.org/10.1016/j.energy.2022.125654.

Giampieri, A., Ling-Chin, J., Roskilly, A.P., 2023. Techno-economic assessment of offshore wind-to-hydrogen scenarios: a UK case study. Int. J. Hydrogen Energy. https://doi.org/10.1016/j.ijhydene.2023.01.346.

Goldmeer, J., 2019. Power to Gas: Hydrogen for Power Generation Fuel Flexible Gas Turbines as Enablers for a Low or Reduced Carbon Energy Ecosystem.

Grainger, D., Bindingsbø, A.U., Brekke, O., De Koeijer, G., Rekaa Nilssen, O., Pettersen, J., 2021. Reducing CO2 emissions from offshore oil and gas production. SSRN Electron. J. https://doi.org/10.2139/ssrn.3820726.

Grasso, M., 2019. Oily politics: a critical assessment of the oil and gas industry's contribution to climate change. Energy Res. Social Sci. 50, 106–115. https://doi.org/10.1016/j.erss.2018.11.017.

GREENSTAT. Optimal utnyttelse av energi fra havvind i Sørlige Nordsjø II Offshore H2-produksjon og kabel til land. May 6, 2023. https://api.greenstat.no/uploads/optimal_utnyttelse_av_energi_fra_havvind_i_sorlige_nordsjo_ii_hr_tn_a20d9e91a9.pdf?updated_at=2022-10-06T14:26:19.192Z.

Hachem, J., Schuhler, T., Orhon, D., Cuif-Sjostrand, M., Zoughaib, A., Molière, M., 2022. Exhaust gas recirculation applied to single-shaft gas turbines: an energy and exergy approach. Energy 238, 121656. https://doi.org/10.1016/j.energy.2021.121656.

Haszeldine, R.S., Flude, S., Johnson, G., Scott, V., 2018. Negative emissions technologies and carbon capture and storage to achieve the Paris Agreement commitments. Phil. Trans. Math. Phys. Eng. Sci. 376 (2119), 20160447 https://doi.org/10.1098/rsta.2016.0447.

International Energy Agency, 2020. The Oil and Gas Industry in Energy Transitions.

International Energy Agency, 2022. Norway 2022 energy policy review. August. 26, 2023. https://iea.blob.core.windows.net/assets/de28c6a6-8240-41d9-9082-a5dd65d9f3eb/NORWAY2022.pdf.

International Renewable Energy Agency (IRENA), 2019. Climate Change and Renewable Energy National Policies and the Role of Communities, Cities and Regions. August. 26, 2023, [Online]. https://www.mofa.go.jp/files/000498436.pdf.

Jing, L., Zhao, T., Wang, Y., Zhou, J., 2022. Modeling and simulation of offshore oil and gas platform AC/DC hybrid microgrid. In: 2022 4th International Conference on Smart Power & Internet Energy Systems (SPIES). IEEE, pp. 1439–1444. https://doi.org/10.1109/SPIES55999.2022.10082439.

Kopp, M., Coleman, D., Stiller, C., Scheffer, K., Aichinger, J., Scheppat, B., Mainz, Energiepark, 2017. Technical and economic analysis of the worldwide largest Power-to-Gas plant with PEM electrolysis,". Int. J. Hydrogen Energy 42 (19), 13311–13320. https://doi.org/10.1016/j.ijhydene.2016.12.145.

Korpås, M., Warland, L., He, W., Tande, J.O.G., 2012. A case-study on offshore wind power supply to oil and gas rigs. Energy Proc. 24, 18–26. https://doi.org/10.1016/j.egypro.2012.06.082.

Kumar, S., Baalisampang, T., Arzaghi, E., Garaniya, V., Abbassi, R., Salehi, F., 2023. Synergy of green hydrogen sector with offshore industries: opportunities and challenges for a safe and sustainable hydrogen economy. J. Clean. Prod. 384, 135545 https://doi.org/10.1016/j.jclepro.2022.135545.

Li, C., Fosso, O.B., Molinas, M., Jingpeng, Y., Raboni, P., 2020. Defining three distribution system scenarios for microgrid applications. In: 2020 IEEE 4th Conference on Energy Internet and Energy System Integration (EI2), pp. 982–987. https://doi.org/10.1109/EI250167.2020.9347144.

Li, C., Othman, M., Ahamad, N.B., Molinas, M., 2022. Marine integrated energy microgrids. In: 2022 International Conference on Renewable Energies and Smart Technologies (REST), pp. 1–5. https://doi.org/10.1109/REST54687.2022.10022621.

Li, Z., Sui, H., Zhang, R., Wang, G., Cai, H., 2023. Short-circuit fault detection scheme for DC microgrids on offshore platforms. Journal of Power Electronics 23 (5), 839–849. https://doi.org/10.1007/s43236-023-00621-3.

Lim, Y.J., Goh, K., Kurihara, M., Wang, R., 2021. Seawater desalination by reverse osmosis: current development and future challenges in membrane fabrication – a review. J. Membr. Sci. 629, 119292 https://doi.org/10.1016/j.memsci.2021.119292.

Luo, J., et al., 2023. Advances in subsea carbon dioxide utilization and storage. Energy Rev. 2 (1), 100016 https://doi.org/10.1016/j.enrev.2023.100016.

Norwegian Meteorological Institute, 2022. Norwegian Meteorological Institute: MEPS Archive, MET Norway Thredds Service.

Norwegian Petroleum Directorate, 2023. Emissions to Air https://www.norskpetroleum.no/en/environment-and-technology/emissions-to-air/#:~:text=In%202022%2C%20greenhouse%20gas%20emissions,Norway's%20aggregate%20greenhouse%20gas%20emissions July. 24, 2023.

Norwegian Petroleum Directorate Professor Olav Hanssens vei, 2020. KraftFraLand to the Norwegian Continental Shelf. Stavanger. May 04, 2023. [Online]. https://www.regjeringen.no/contentassets/f189f2bbba3d42f8be6578371e30eac0/kraft-fra-land-til-norsk-sokkel-2020.pdf.

Oliveira-Pinto, S., Rosa-Santos, P., Taveira-Pinto, F., 2019. Electricity supply to offshore oil and gas platforms from renewable ocean wave energy: overview and case study analysis. Energy Convers. Manag. 186, 556–569. https://doi.org/10.1016/j.enconman.2019.02.050.

Panda, D.K., Das, S., 2021. Smart grid architecture model for control, optimization and data analytics of future power networks with more renewable energy. J. Clean. Prod. 301, 126877 https://doi.org/10.1016/j.jclepro.2021.126877.

Peters, R., Vaessen, J., van der Meer, R., 2020. Offshore hydrogen production in the North Sea enables far offshore wind development. In: Day 4 Thu, May 07, 2020. OTC. https://doi.org/10.4043/30698-MS.

Polleux, L., Guerassimoff, G., Marmorat, J.-P., Sandoval-Moreno, J., Schuhler, T., 2022. An overview of the challenges of solar power integration in isolated industrial microgrids with reliability constraints. Renew. Sustain. Energy Rev. 155, 111955 https://doi.org/10.1016/j.rser.2021.111955.

Riboldi, L., Alves, E.F., Pilarczyk, M., Tedeschi, E., Nord, L.O., 2020. Optimal design of a hybrid energy system for the supply of clean and stable energy to offshore installations. Front. Energy Res. 8 https://doi.org/10.3389/fenrg.2020.607284.

Roussanaly, S., et al., 2019. Offshore power generation with carbon capture and storage to decarbonise mainland electricity and offshore oil and gas installations: a techno-economic analysis. Appl. Energy 233 (234), 478–494. https://doi.org/10.1016/j.apenergy.2018.10.020.

Shezan, Sk A., et al., 2023. Evaluation of different optimization techniques and control strategies of hybrid microgrid: a review. Energies 16 (4), 1792. https://doi.org/10.3390/en16041792.

Stuen, T.H., 2021. Influence of Hydrogen Use as a Fuel on Aeroderivative Gas Turbine Performance. Norwegian University of Science and Technology.

Sundsbø Alne, K., 2007. Reduction of NOx Emissions from the Gas Turbines for Skarv Idun. Masters, Norwegian University of Science and Technology, Trondheim.

Svendsen, H.G., Holdyk, A., Vrana, T.K., Mosgren, I.R., Wiik, J., 2022. Operational planning and power management system for offshore platform with wind energy supply – impacts on CO2 reduction and power quality. In: Petroleum Technology, 10. American Society of Mechanical Engineers. https://doi.org/10.1115/OMAE2022-78802.

Tampen - Equinor, Hywind. April. 17, 2023. https://www.equinor.com/energy/hywind-tampen.

Tan, W., Zhang, A., Feng, Y., Sun, Y., huang, H., Siyuan, W., 2019. Study on short-term load forecasting method considering meteorological factors of offshore oilfield group microgrid. In: 2019 IEEE Innovative Smart Grid Technologies - Asia. ISGT Asia), pp. 850–853. https://doi.org/10.1109/ISGT-Asia.2019.8881350.

Tangerås, B.-T., Tveiten, Å.S., 2018. Hywind Tampen, Project NPV Calculation with and without Subsidies.

Tilocca, G., S'anchez, D., Torres Garc'ıa, M., Escamilla Perejon, A., 2023. A methodology to quantify product competitiveness and innovation requirements for micro gas turbine systems in hydrogen backup applications. In: ASME Turbo Expo 2023: Turbomachinery Technical Conference and Exposition. ASME Turbo Expo, Boston.

Ventrelli, S., 2022. Combining renewable microgrids and energy storage: decarbonizing offshore assets by means of offshore floating solar and wind. In: Day 1 Mon, October 31, 2022. SPE. https://doi.org/10.2118/210821-MS.

Watson, S.M., 2020. Greenhouse gas emissions from offshore oil and gas activities — relevance of the Paris agreement, law of the sea, and regional seas programmes. Ocean Coast Manag. 185, 104942 https://doi.org/10.1016/j.ocecoaman.2019.104942.

Wu, J., Chen, X.-Y., Zhang, H., Xiong, L.-D., Lei, H., Deng, S.-H., 2019. Hyperparameter optimization for machine learning models based on bayesian optimizationb. Journal of Electronic Science and Technology 17 (1), 26–40. https://doi.org/10.11989/JEST.1674-862X.80904120.

Yu, Q., Liu, Y., Li, D., Jiang, Z., Long, G., 2020. Research of SSO and suppression method of distributed micro grid in offshore oil platform. In: 2020 39th Chinese Control Conference (CCC). IEEE, pp. 6214–6218. https://doi.org/10.23919/CCC50068.2020.9188859.

Zare, P., Davoudkhani, I.F., Zare, R., Ghadimi, H., Mohajeri, R., Babaei, A., 2023. Maiden application of zebra optimization algorithm for design PIDN-TIDF controller for frequency control in offshore fixed platforms microgrid in the presence of tidal energy. In: 2023 8th International Conference on Technology and Energy Management (ICTEM), IEEE, Feb, pp. 1–7. https://doi.org/10.1109/ICTEM56862.2023.10083612.

Zhang, Q., Ogren, R.M., Kong, S.-C., 2018. Thermo-economic analysis and multi-objective optimization of a novel waste heat recovery system with a transcritical CO2 cycle for offshore gas turbine application. Energy Convers. Manag. 172, 212–227. https://doi.org/10.1016/j.enconman.2018.07.019.

Zhang, Q., et al., 2021. Sustainable and clean oilfield development: how access to wind power can make offshore platforms more sustainable with production stability. J. Clean. Prod. 294, 126225 https://doi.org/10.1016/j.jclepro.2021.126225.
Carbon Capture and Storage - Norwegianpetroleum.No, 2023. August. 20, 2023. [Online]. https://www.norskpetroleum.no/en/environment-and-technology/carbon-capture-and-storage/.
Hydrogen - TechnipFMC plc. https://www.technipfmc.com/en/what-we-do/new-energy/hydrogen/. May 6, 2023.
Hywind Tampen approved by Norwegian authorities - equinor.com." https://www.equinor.com/news/archive/2020-04-08-hywind-tampen-approved (accessed June. 11, 2023).
Tax rates in Norway." https://www.regjeringen.no/no/tema/okonomi-og-budsjett/skatter-og-avgifter/avgiftssatser-2023/id2929584/(accessed May 3, 2023).
Views from the industry: equinor. June. 16, 2023. https://www.dnv.com/cases/views-from-the-industry-equinor-183622.